Research Journal of Applied Sciences, Engineering and Technology 5(18): 4510-4517, 2013
DOI:10.19026/rjaset.5.4366
ISSN: 2040-7459; e-ISSN: 2040-7467

Submitted: October 17, 2012 Accepted: January 03, 2013 Published: May 05, 2013

Research Article

Research on a Novel Soft-Switching Buck Converter

[1, 2]Yuanbin Li, [1]Peng Ge and [2]Ben Niu
[1]Hangzhou Non-Commissioned Officer Academy of CAPF, Hangzhou 310023, China
[2]College of Civil Aviation, Nanjing University of Aeronautics and Astronautics, Nanjing 210016, China

Abstract: Based on classical zero voltage transition buck pwm converter, an ideal buck converter with pwm-controlled soft-switching circuit is proposed. The proposed auxiliary circuit allows the main switch to operate with zero-voltage switching. Besides, all of the semiconductor devices operate under soft-switching conditions. Thus, losses were reduced. It was analyzed in detail to demonstrate the operating principle of the novel circuit. Finally, simulation results are given analysis and the simulation results are provided to verify the performance of the proposed buck Converter.

Keywords: Buck converter, resonance, soft-switching, zero voltage transition

INTRODUCTION

Recent years, as the interest increased by the industry in power converters with high frequency and small size, lots of novel topologies have been proposed in literatures (Martins *et al*., 2005; Lin *et al*., 2010). With the switching frequency increase, high power density can be achieved. But under the hard switching condition, the di/dt and du/dt is large during the communication process. So soft-switching technique is developed and some was employed to the power converters, usually auxiliary components are used (Wu *et al*., 2008; Li *et al*., 2010). In the last years, researchers paid more attention to Zero Voltage Transition (ZVT), which is the voltage-mode soft-switching method (Seyed *et al*., 2008). The operation of ZVT is similar to PWM converters and its additional conductions have low losses (Adib and Farzanehfard, 2009; Iannuzzo, 2005). The location of auxiliary circuit causes these remarkable features and the auxiliary circuit is placed in parallel with the main power converter. Before the main switch is turned on, the auxiliary circuit works, when the main switch is turned off, the auxiliary circuit ceases (Martins *et al*., 2005). In that way, the additional conduction losses are mostly reduced. Moreover, the operation characteristics have few influences. Previously proposed ZVT-PWM converters have at least one of the following drawbacks (Panda *et al*., 2008):

- The auxiliary switch is turned off while it is conducting current. That causes the switching losses
- The main converter switch operates with a higher peak current stress and/or voltage stress
- The auxiliary circuit components have high voltage and/or current stress
- Some circuits are complex, difficult to control and so on.

This study presents a novel ZVT buck converter by using a resonant auxiliary network. And the proposed converter achieves zero-voltage switching for the main switching and zero-current switching for the auxiliary switching.

THE NOVEL SOFT-SWITVHING BUCK CONVERTER

Circuit description and assumption: The proposed novel soft-switching buck converter is show in Fig. 1. It is the combination of the conventional PWM buck converter and the proposed auxiliary snubber circuit. The auxiliary circuit consists of a resonant inductor L_r, resonant capacitor C_r, C_1, C_2, three auxiliary diodes VD_1, VD_2, VD_3 and auxiliary switching VT_2.

The following assumptions are made during one switching cycle in order to analyze the steady-state operations of the proposed circuit.

- Input voltage U_i is constant
- Output voltage U_o is constant or output capacitor C_o is large enough
- Output current I_o is constant or output inductor L_o is large enough
- Output inductor L_o is much larger than resonant circuit inductor L_r
- Resonant circuits are ideal
- Semiconductor devices are ideal

Corresponding Author: Ben Niu, College of Civil Aviation, Nanjing University of Aeronautics and Astronautics, Nanjing 210016, China

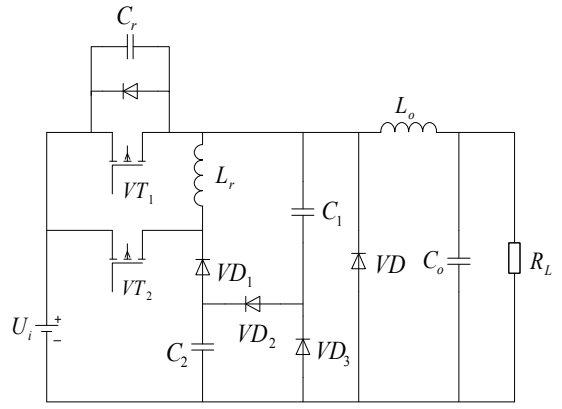

Fig. 1: The proposed novel soft-switching buck converter

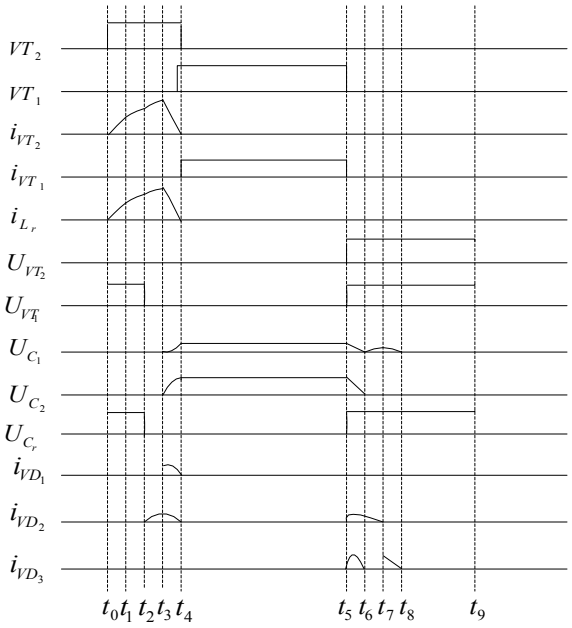

Fig. 2: Key theoretical waveforms of the proposed converter

Reverse recovery time of all diodes is ignored

Operation principles and analysis: Based on the assumptions above, circuit operation in one switching cycle can be divided into nine stages. The key waveforms are shown in Fig. 2 and the equivalent circuit of the operation stages is shown in Fig. 3. The detailed analysis of every stage will be discussed in the following paragraphs.

Mode 1($t_0 \sim t_1$): Prior to t_0, the main diode VD is conducting, while the main switching VT_1 and the auxiliary switching VT_2 were off. At the beginning of this stage:

$$i_{VT_1} = 0\ i_{VT_2} = 0\ i_{L_r} = 0\ U_{C_1} = 0\ U_{C_2} = 0\ i_D = I_o\ U_{C_r} = U_i$$

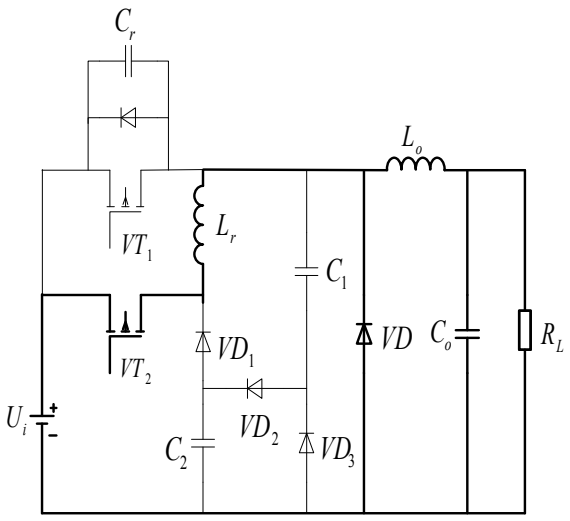

(a) mode 1($t_0 \sim t_1$)

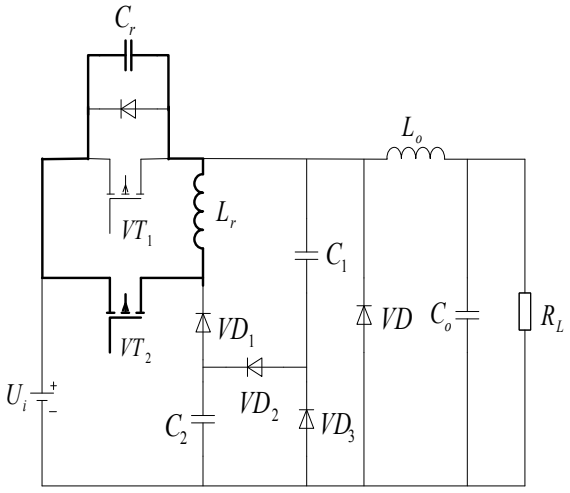

(b) mode 2($t_1 \sim t_2$)

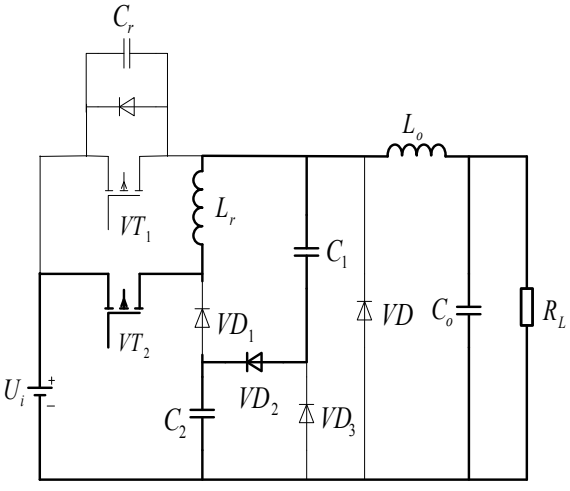

(c) mode 3($t_2 \sim t_3$)

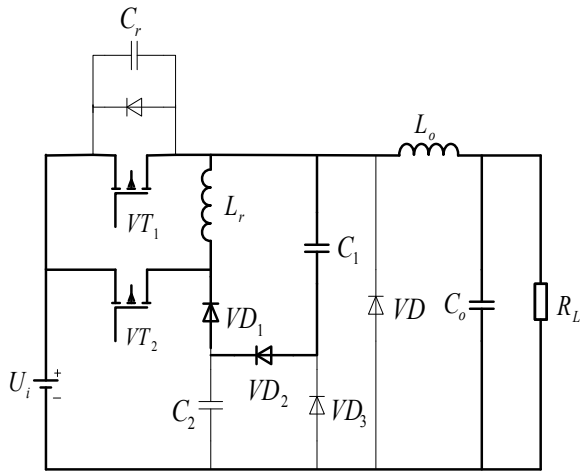

(d) mode 4($t_3 \sim t_4$)

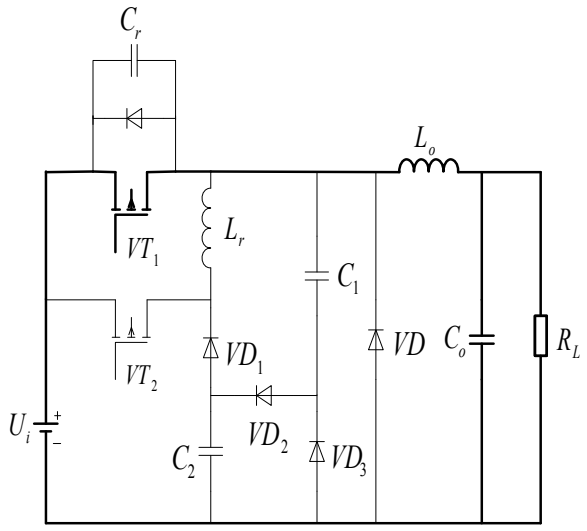

(e) mode 5($t_4 \sim t_5$)

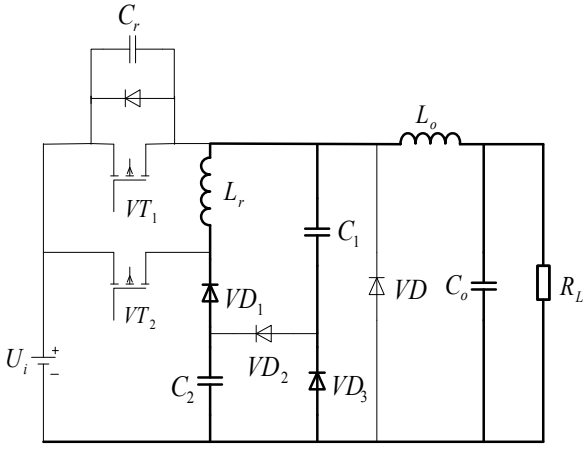

(f) mode 6($t_5 \sim t_6$)

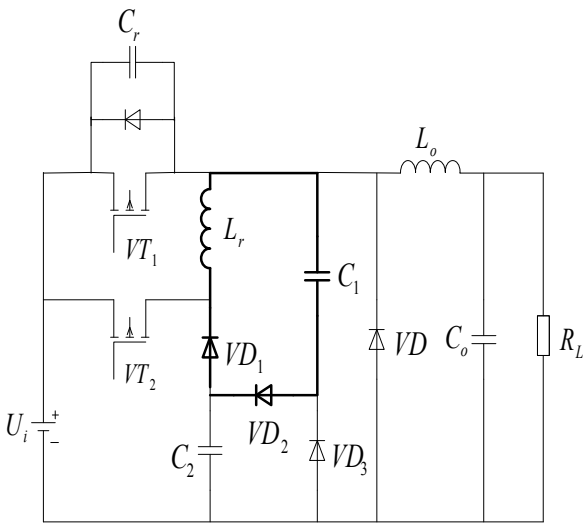

(g) mode 7($t_6 \sim t_7$)

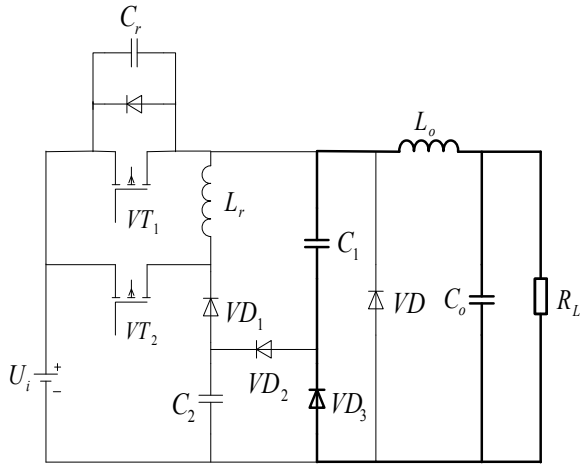

(h) mode 8($t_7 \sim t_8$)

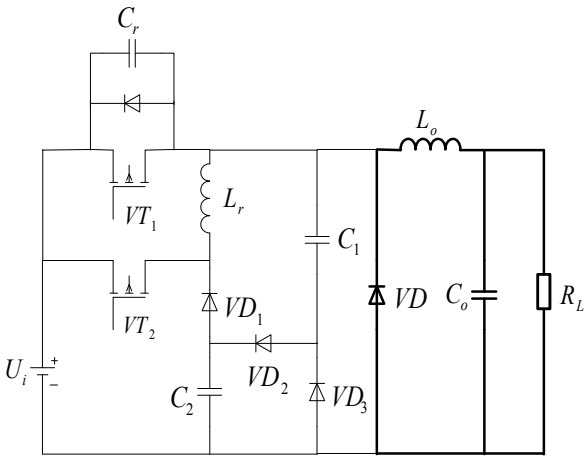

(i) mode 9($t_8 \sim t_9$)

Fig. 3: The equivalent circuit of the operation stages

At $t = t_0$, the auxiliary switching VT_2 is turned on, which realizes zero-current turn-on as it is in series with the resonant inductor L_r. During this stage, i_{L_r} rises and the current of the main diode fall simultaneously at the same rate linearly. This mode ends at t = t_1 when i_{L_r} reaches I_o and i_D becomes zero. The main diode VD is turned off with ZVS because of C_1 and C_2 being existent. In this state,

$$i_{VT_2} = i_{L_r} = \frac{U_i}{L_r}(t - t_0) \tag{1}$$

$$i_D = I_o - \frac{U_i}{L_r}(t - t_0) \tag{2}$$

$$t_{01} = \frac{L_r}{U_i} I_o \tag{3}$$

Mode 2 ($t_1 \sim t_2$): The diode VD_2 starts conducting with ZVS at the instant when the main diode VD is turned off. At

$$t = t_1, i_{VT_1} = 0, i_{VT_2} = I_o, i_{L_r} = I_o, U_{C_1} = 0, U_{C_2} = 0,$$
$$i_D = 0, U_{C_r} = U_i$$

In this interval, resonance occurs with the inductor L_r and the capacitor C_r, i_{L_r} increases on and U_{C_r} falls, at the end of this mode, the voltage of the capacitor C_r falls to zero:

$$i_{L_r}(t) = I_o + \frac{U_i}{Z}\sin\omega(t - t_1) \tag{3}$$

$$U_{C_r}(t) = U_i \cos(t - t_1) \tag{4}$$

where,

$$w = \frac{1}{\sqrt{L_r C_r}} \quad Z = \sqrt{L_r / C_r} \tag{5}$$

At $t = t_2$, $U_{C_r} = 0$ the diode reverse parallelled VT_1 is conducting, it clamps the voltage of the main switching with zero. At this moment:

$$i_{L_r} = I_o + \frac{U_i}{Z} \tag{6}$$

$$t_{12} = \frac{\pi}{2}\sqrt{L_r C_r} \tag{7}$$

Mode 3($t_2 \sim t_3$): At $t = t_2$, $i_{VT_1} = 0$, $i_{VT_2} = I_o$, $i_{L_r} = I_o + \frac{U_i}{Z}$, $U_{C_1} = 0$, $U_{C_2} = 0$, $i_D = 0$, $U_{C_r} = 0$.

The current of the resonance inductor flows through the diode which reverse paralleled VT_1 and the main switching VT_1 turns on with ZVS. And the time when VT_1 turns on is later than the time VT_2 turns on.
The delayed time:

$$t_d \geq t_{01} + t_{12} = \frac{L_r}{U_i} I_o + \frac{\pi}{2}\sqrt{L_r C_r} \tag{8}$$

In this interval, resonance occurs with the inductor L_r and capacitor C_1 and C_2.This mode ends with C_2 is charged up to the input voltage U_i:

$$U_{C_2}(t) = \frac{C_e}{C_2}[U_i - U_i \cos\omega_1(t - t_2)] \tag{9}$$

$$U_{C_1}(t) = \frac{C_e}{C_1}[U_i - U_i \cos\omega_1(t - t_2)] \tag{10}$$

$$i_{L_r}(t) = \frac{U_i}{Z_1}\sin\omega_1(t - t_2) + \frac{U_i}{Z} + I_o \tag{11}$$

where,

$$C_e = \frac{C_1 C_2}{C_1 + C_2}$$
$$\omega_1 = \frac{1}{\sqrt{L_r C_e}} \tag{12}$$
$$Z_1 = \sqrt{L_r / C_e}$$

When the U_{C_2} becomes U_i, the diode VD_1 is turned on with ZVS. In this state:

$$t_{23} = \frac{1}{\omega_1}\arccos\left(1 - \frac{C_2}{C_e}\right) \tag{13}$$

Mode 4($t_3 \sim t_4$): At $t = t_3, i_{VT_1} = I_o, i_{Lr} = i_{Lr\max}$, $U_{C_2} = U_i$, $U_{C_1} = U_{C_1 1}$.When VD_1 turns on, new resonance starts with L_r and C_1, and C_1 is charged up:

$$U_{C_1}(t) = I_{L_r \max} Z_2 \sin\omega_2(t - t_3) + U_{C_1 1}\cos\omega_2(t - t_3) \tag{14}$$

$$i_{L_r}(t) = I_{L_r \max} Z_2 \sin\omega_2(t - t_3) - \frac{U_{C_1 1}}{Z_2}\sin\omega_2(t - t_3) \tag{15}$$

where,

$$\omega_2 = \frac{1}{\sqrt{L_r C_1}} \quad Z_2 = \sqrt{L_r / C_1} \tag{16}$$

This mode ends when C_1 is charged up to its maximum voltage $U_{C_1 2}$. Diodes VD_1 and VD_2 are turned off with ZCS due to the existence of L_r. And at the same time, auxiliary switching VT_2 turns off with ZCS. In this state:

$$t_{34} = \frac{1}{\omega_2}\arctan\left(\frac{I_{L_r \max} Z_2}{U_{C_1 1}}\right) \tag{17}$$

Mode 5 ($t_4 \sim t_5$): There is no resonance in this mode and the circuit operation is identical to that of a conventional PWM buck converter:

$$i_{VT_1} = I_o \tag{18}$$

Mode 6($t_5 \sim t_6$): At $t = t_5$, $i_{VT_1} = I_o$, $i_{L_r} = 0$, $U_{C_2} = U_i$, $U_{C_1} = U_{C_1 2}$. The main switching VT_1 is turned off under ZVS because the voltage of the capacitor C_r cannot rise suddenly. C_1 is clamped to zero. Resonance occurs with L_r and C_2. The voltage and current equations for this mode are:

$$i_{L_r}(t) = \frac{U_i}{Z_3}\sin\omega_3(t - t_5) \tag{19}$$

$$U_{C_1}(t) = 0 \tag{20}$$

$$U_{C_2}(t) = U_i \cos\omega_3(t - t_5) \tag{21}$$

$$t_{56} = \frac{1}{\omega_3}\frac{\pi}{2} = \frac{\pi}{2}\sqrt{L_r C_2} \tag{22}$$

where,

$$Z_3 = \sqrt{L_r / C_2} \quad \omega_3 = \frac{1}{\sqrt{L_r C_2}} \tag{23}$$

This mode ends when the voltage across C_2 becomes zero.

Mode 7($t_6 \sim t_7$): At $t = t_6, U_{C_1} = 0, U_{C_2} = 0$, $i_{L_r} = i_{L_r 1} = \frac{U_i}{Z_3}$

The diode VD_2 turns on under ZVS. Resonance starts with inductor L_r and C_1 capacitor C_1. And C_1 is charged up. For this state, the equations are:

$$U_{C_1}(t) = I_{L_r 1} Z_2 \sin\omega_2(t - t_6) \tag{24}$$

$$i_{L_r}(t) = I_{L_r 1}\cos\omega_2(t - t_6) \tag{25}$$

$$\omega_2 = \frac{1}{\sqrt{L_r C_1}} \quad Z_2 = \sqrt{L_r / C_1} \tag{26}$$

When i_{L_r} becomes zero, this mode comes to an end. The time interval for this mode is given as:

$$t_{67} = \frac{\pi}{2}\frac{1}{\omega_2} = \frac{\pi}{2}\frac{1}{\sqrt{L_r C_1}} \tag{27}$$

Mode 8 ($t_7 \sim t_8$): At $t = t_7\ U_{C_1} = U_{C_1 3}\ U_{C_2} = 0\ i_{L_r} = 0$ $i_{VT_1} = 0\ i_{VT_2} = 0$

The stored energy of capacitor C1 is now transferred to load.

Mode 9($t_8 \sim t_9$): At $t = t_8$, the main diode VD is conducting under ZVS, the load current will flow through the main diode VD. During this mode, the converter operates like a conventional PWM buck converter until the auxiliary switching VT_2 is turned on in the next switching cycle. In this mode:

$$i_D = I_o \tag{28}$$

DESIGN PROCEDURE

The proposed converter operates with an input voltage $U_i = 200V$, output voltage $U_o = 80V$, load current of 20A and the switching frequency of 20kHz.. The following design procedure is developed considering procedure of literatures (Zhang *et al*., 2007).

- Selection of the resonant inductor L_r. From the analysis of mode 1, the speed of the current flowing through L_r increases fast if the resonant inductor L_r is too small, thus it can't limit the reverse current of the main diode VD. And from the analysis of mode 2, if the resonant inductor L_r is too small, ΔI_{L_r} will be very large, which may increase the turn-on losses of the auxiliary switching VT_2. In the designations, it is considered as followings:
  $\Delta t_1 = t_1 - t_0 = 0.01DT_s$. In this case, from (1):

$$L_r = \frac{U_i}{i_{L_r}(t_1)}\Delta t_1 = \frac{0.01DT_s U_i}{I_o} \tag{29}$$

- Selection of C_r, C_1, C_2. In order to provide ZVS turn-on for the main switching VT_1, the energy of C_r should transform to L_r, considering

$$\frac{1}{2}C_r U_{C_r}^2 = \frac{1}{2}C_r U_i^2 = \frac{1}{2}L_r \Delta I_{L_r}^2 \tag{30}$$

$$C_r = \frac{L_r \Delta I_{L_r}^2}{U_i^2} \tag{31}$$

The capacitor C_2 will transform the energy to L_r at least the time period t_f during the turn off of the main switching, according to formula (22):

$$t_{56} = \frac{1}{\omega_3}\frac{\pi}{2} = \frac{\pi}{2}\sqrt{L_r C_2} \geq t_f \tag{32}$$

t_f is the fall time of the main switching.
With the energy balance defined as:

$$\frac{1}{2}C_2 U_i^2 + \frac{1}{2}C_1 U_{C_1}^2 = \frac{1}{2}L_r I_{o\max}^2 \tag{33}$$

The capacitor C_1 can be calculated.

SIMULATION RESULTS

The converter is simulated using simulation software OrCad, version 10.5. The major parameters are given as follows:

$$L_r = 3uH \;\; C_r = 0.3nF \;\; C_1 = 80nF \;\; C_2 = 23nF$$
$$U_i = 200V \;\; U_o = 80V \;\; I_o = 20A \;\; f_s = 20kHz$$

Figure 4 depicts the drive waveforms of main and auxiliary switching when the main switching's duty cycles is 0.4 and Fig. 5 depicts the drive waveforms of main and auxiliary switching with 0.8 duty cycles of the main switching. The waveforms of current and voltage on main switching with 0.4 duty cycles of the main switching is shown in Fig. 6, when the voltage of main switching falls to zero, the current then increases. And before the voltage increases, the current falls to zero. So the power loss is nearly to zero, the main switching achieves zero-voltage switching. Figure 7 describes the waveforms of current and voltage on auxiliary

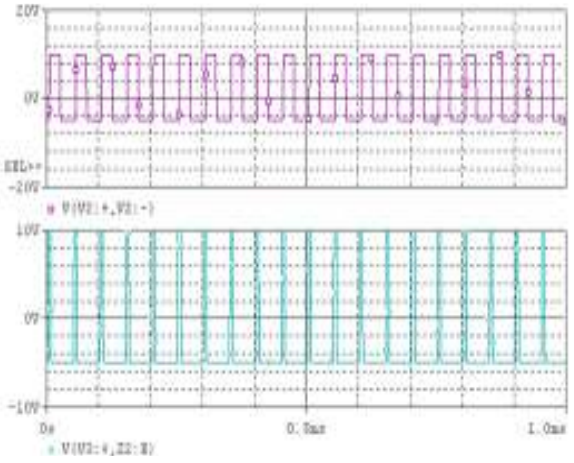

Fig. 4: The drive waveforms of main and auxiliary switching at 0.4 duty cycle of the main switching

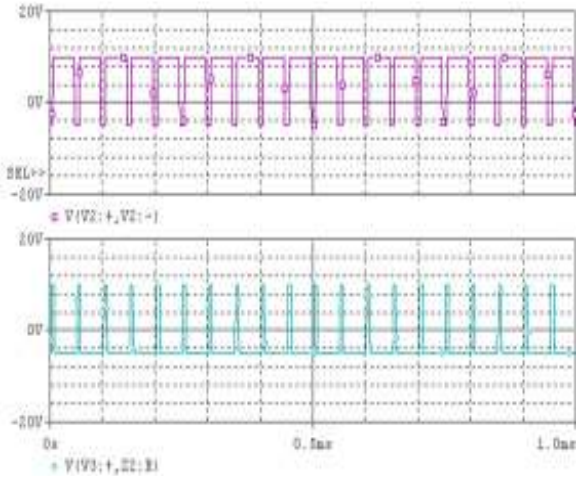

Fig. 5: The drive waveforms of main and auxiliary switching at 0.8 duty cycle of the main switching

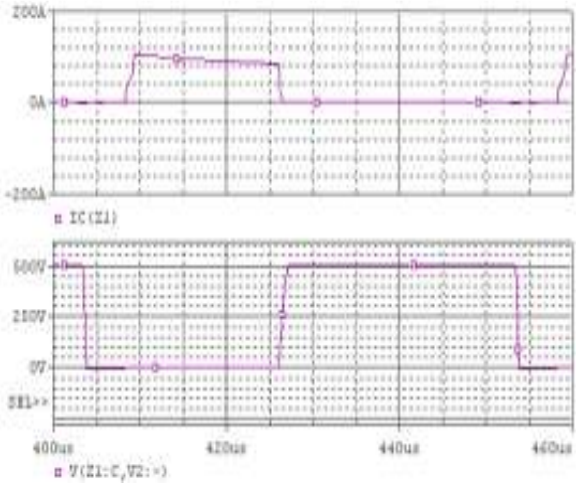

Fig. 6: The waveforms of current and voltage of main switching at 0.4 duty cycle

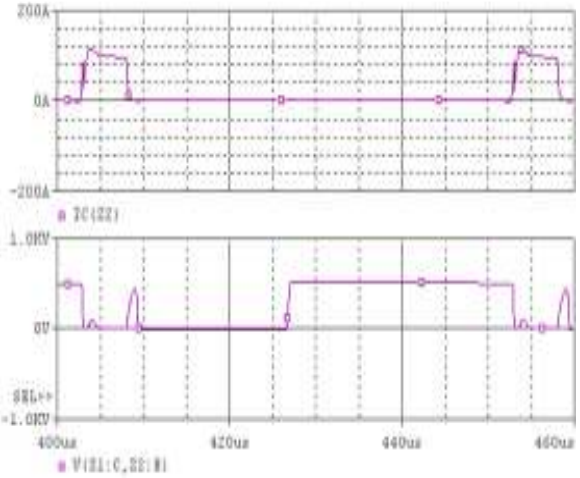

Fig. 7: The waveforms of current and voltage of auxiliary switching at 0.4 duty cycle

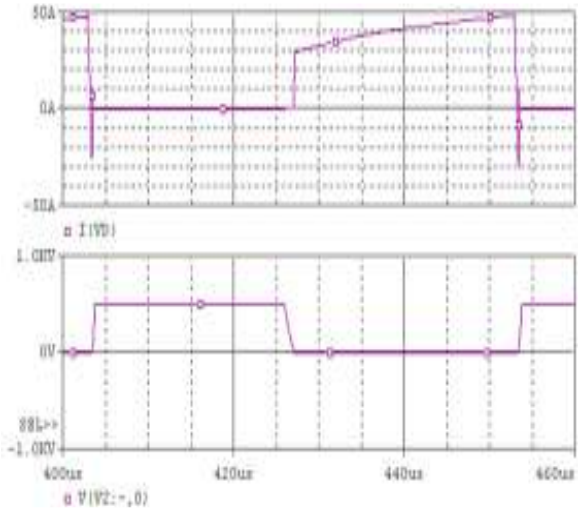

Fig. 8: The waveforms of current and voltage of main diode at 0.4 duty cycle

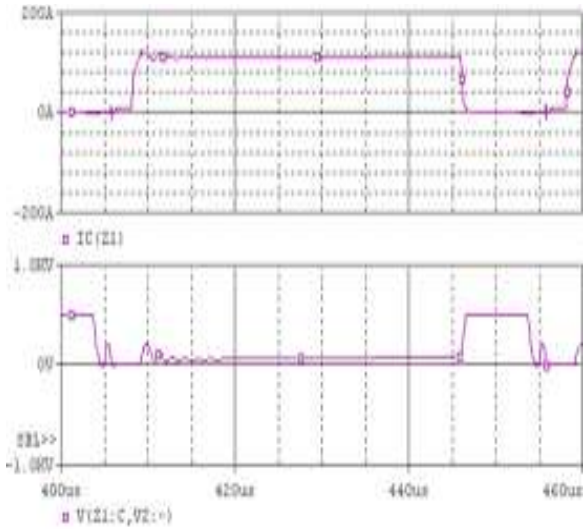

Fig. 9: The waveforms of current and voltage of main switching at 0.8 duty cycle

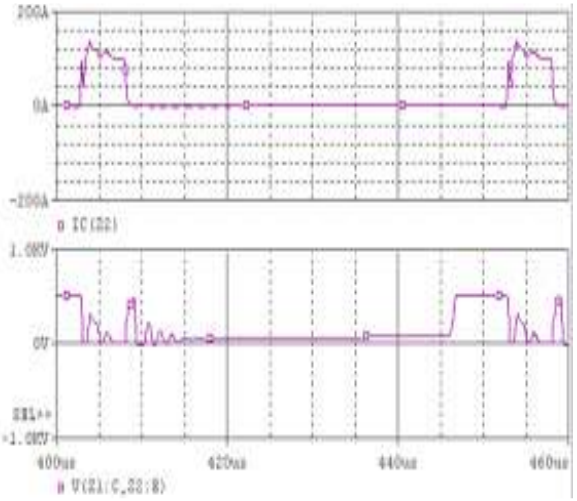

Fig. 10: The waveforms of current and voltage of auxiliary switching at 0.8 duty cycle

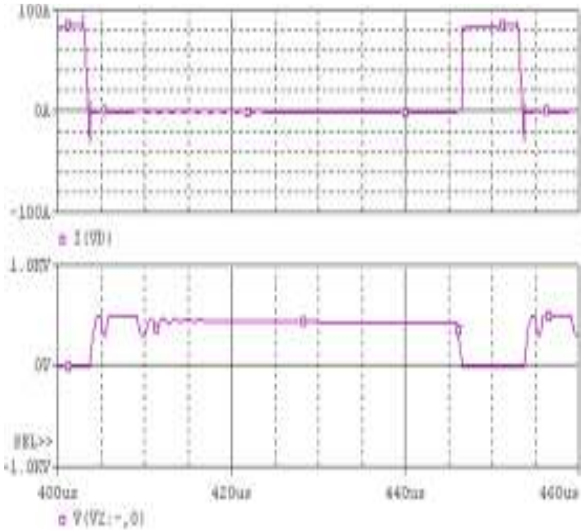

Fig. 11: The waveforms of current and voltage of main diode at 0.8 duty cycle

switching with 0.4 duty cycles of the main switching, before the current of auxiliary switching increases, the voltage has decreased to zero and the voltage increases after the current has decreased to zero. Thus the current of auxiliary achieves zero-current switching and the power loss is reduced. But when the current decreases to zero, there is a fluctuation of voltage. Figure 8 presents the main diode turns on and off under soft-switching conditions with 0.4 duty cycles of the main switching. Figure 9 depicts the waveforms of current and voltage on main switching with 0.8 duty cycle of main switching. Figure 10 describes the waveforms of current and voltage on auxiliary switching with 0.8 duty cycle of main switching. And Fig. 11 presents the waveforms of current and voltage on main diode with 0.8 duty cycle of main switching. As the figures shown, when the duty cycle of main switching increases, there is a small fluctuation of voltage, but it has little influence in the circuit.

CONCLUSION

As the simulation results shown, the main switching turns on and off with ZVS. And the auxiliary switching ZCS turns on and turns off. All the diodes operate under soft-switching conditions. Switching losses are reduced. And the additional voltage and current stresses on the main devices do not take place. The proposed circuit can also be used in the vehicle voltage converter, which the author will develop further research next step.

REFERENCES

Adib, E. and H. Farzanehfard, 2009. Soft switching bidirectional DC-DC converter for ultracapacitor-batteries interfaces. Energ. Convers. Manage., 50: 2879-2884.

Iannuzzo, F., 2005. Non-destructive testing technique for MOSFET's characterisation during soft-switching ZVS operations. Microelectr. Reliab., 45: 1738-1741.

Li, S., X. Zhou, X. Chen and Q. Gan, 2010. Designing a compact soft-start scheme for voltage-mode DC–DC switching converters. Microelectr. J., 41: 430-439, DOI: 10.1016/j.mejo.2010.05.001.

Lin, S.Z., X.C. Zou, X.F. Chen and Q. Gan, 2010. Designing a compact soft-start scheme for voltage-mode DC-DC switching converters. Microelectr. J., 41: 430-439, DOI: 10.1016/j.mejo.2010.05.001.

Martins, M.L., J.L. Russi and H.L. Hey, 2005. A classification methodology for zero-voltage transition pwm converters. IEEE Proc. Electr. Power Appl., 152: 323-334, DOI: 10.1049/ ipepa:20041230.

Panda, A.K., S. Pattnaik and K.K. Mohapatra, 2008. A novel soft-switching synchronous buck converter for portable applications. Int. J. Power Manage. Electron., DOI: 10.1155/2008/862510.

Seyed, H.H., S. Mehran, Y.G. Ali, 2008. An improved topology of electronic ballast with wide dimming range, PFC and low switching losses using PWM-controlled soft-switching inverter. Electr. Pow. Syst. Res., 78: 975-984, DOI: 10.1016/ j.epsr. 2007.07.006.

Wu, X.K., J.M. Zhang, X. Ye and Z.M. Qian, 2008. Analysis and derivations for a family ZVS converter based on a new active clamp ZVS cell. IEEE T. Ind. Electron., 55: 733-781.

Zhang, W.P., X.Q. Zhang, Z.G. Chen and Y.C. Liu, 2007. A novel soft switching for buck converter. Proceeding of the CSEE, 27: 110-115.